Experimental report

02/10/2019

Proposal: 5-54-224 **Council:** 10/2016

Title: Interface and strain effects on the magnetic properties of manganite multilayers.

Research area: Physics

This proposal is a new proposal

Main proposer: Santiago Jose CARREIRA

Experimental team: Santiago Jose CARREIRA

Local contacts: Alexei VOROBIEV

Samples: LSAT//[La0.67Sr0.33MnO3 (10 nm)/La0.9Sr0.1MnO3 (b nm)]4
STO//[La0.67Sr0.33MnO3 (10 nm)/La0.9Sr0.1MnO3 (b nm)]4

Instrument	Requested days	Allocated days	From	To
D17	7	0		
SUPERADAM	0	7	01/10/2018	08/10/2018

Abstract:

We propose to study the magnetic properties at the interface between different Sr-doped oxide-manganites. An enhancement of the spin polarization at the interface of La0.67Sr0.33MnO3 (LSMO)/La1-xSrxMnO3 (LSxMO) with x≤0.1 has been observed with respect to the conventional system LSMO/SrTiO3 (STO), usually employed in tunneling devices. With PNR experiments at the D17 station we expect to obtain a quantitative description of the magnetic profile throughout the multilayers of S//[La0.67Sr0.33MnO3 (10nm)/La0.9Sr0.1MnO (bnm)]4, where 3nm<b<9nm and S is the substrate, which in this case will be STO and (LaAlO3)0.3(Sr2TaAlO6)0.7 (LSAT). Any magnetic reconstruction inherent to the broken symmetry phenomena at the interfaces will be reflected on the magnetic modulation. In addition, the magnetic profile will be studied in terms of the doping level and for different temperatures. We will also be concern of the effect of the strain induced by different substrates. These experiments will be very useful in order to give an accurate description of the magnetic properties in these strong correlated electron systems.

Interface and strain effects on the magnetic properties of manganite multilayers

Report Proposal 5-54-224

Santiago J. Carreira, [a,b] Myriam H. Aguirre,[c,d,e] Javier Briatico,[f] and Laura B. Steren,[a,b]

[a.] Consejo Nacional de Investigaciones Científicas y Técnicas, Argentina. Tel: 54-11 6772-7103; E-mail: *steren@tandar.cnea.gov.ar.*
[b.] Laboratorio de Nanoestructuras Magnéticas y Dispositivos. Dpto. Materia Condensada e Instituto de Nanociencia y Nanotecnología (INN), Centro Atómico Constituyentes (CNEA), (1650) San Martín, Buenos Aires, Argentina.
[c.] Instituto de Ciencia de Materiales de Aragón (ICMA) e Instituto de Nanociencia de Aragón (INA), Universidad de Zaragoza, E-50018 Zaragoza, Spain. Fax: +34 976 76 2776; Tel: +34 876 55 5365; E-mail: *maguirre@unizar.es*.
[d.] Departamento de Física de la Materia Condensada, Universidad de Zaragoza, E-50009 Zaragoza, Spain.
[e.] Laboratorio de Microscopías Avanzadas, Universidad de Zaragoza, E-50018 Zaragoza, Spain.
[f.] Unité Mixte de Physique, CNRS, Thales, Université Paris-Sud, Université Paris-Saclay, Palaiseau 91767, France.

Abstract

In this report we describe the magnetic properties at the interface between different Sr-doped oxide-manganites multilayers, based on the results obtained at SUPERADAM (Proposal 5-54-224). These results were correlated with a structural and compositional analysis in order to give an accurate description of the magnetic properties in these strong correlated electron systems. The magnetic profile found for the reference multilayer STO//[$La_{0.7}Sr_{0.3}MnO_3$ (10 nm)/$SrTiO_3$ (6 nm)]x4 ($LS_{0.3}$MO/STO) reveals non symmetrical interfaces and larger interfacial magnetization for the STO/$LS_{0.3}$MO interfaces with respect to the $LS_{0.3}$MO /STO ones. Moreover, the magnetic profile correlates fairly well with the local oxidation states throughout the structure. The replacement of the STO by the un-doped manganite $LaMnO_3$ gives rise to a more symmetrical magnetic.

Data process and experimental results

Two types of multilayers were grown by pulsed laser deposition over STO (001) substrates. The first with nominal composition STO//[$LS_{0.3}$MO (10 nm)/STO (6 nm)]x4 (ML_{STO}) was used as a reference and a modified multilayer with nominal composition STO//[$LS_{0.3}$MO (10 nm)/LMO (6 nm)]x4 (ML_{LMO}) was employed to test the interfacial modifications. The overall magnetic moment and Curie temperature of both samples were extracted from the temperature dependent magnetization measurements performed with an MPMS-SQUID, as shown in Fig. 1(a).

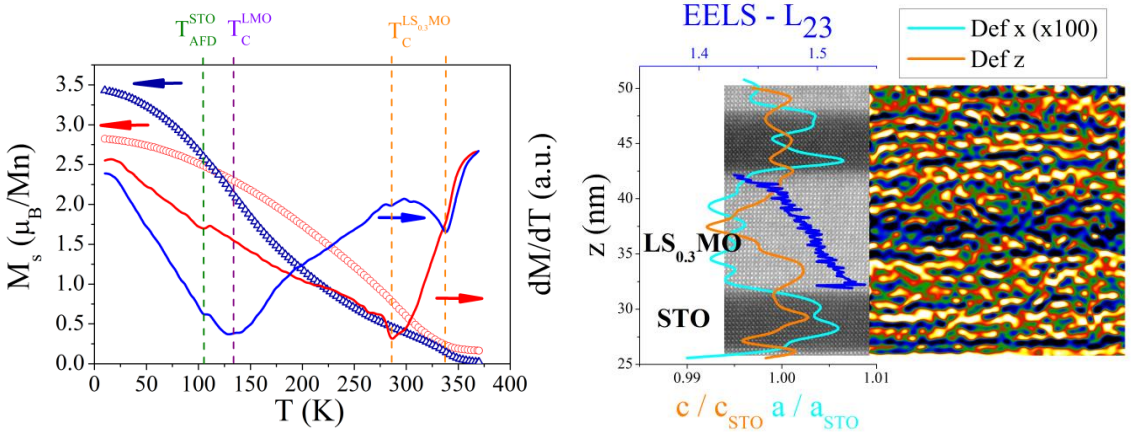

Fig. 1: (b) Magnetization M_S (right axis) and derivative dM_S/dT (left axis) of the ML_{STO} (red) and ML_{LMO} (blue). The temperatures T_{AFD}^{STO}, T_C^{LMO} and $T_C^{LS_{0.3}MO}$ correspond to the antiferrodistortive transition of the STO and the Curie temperature of the LMO and $LS_{0.3}$MO respectively. (b) HAADF-STEM image and GPA out of plane strain map for the sample ML_{STO}. The graph shows the depth profile of the calculated ratio of the out of plane lattice parameters c / c_{STO} and in plane parameters a / a_{STO}, extracted from the GPA analysis. Superimposed to the STEM image we plotted the depth profile of the L_{23} calculated from the EELS scans.

In order to simplify the comparison between samples, in both cases the magnetization was normalized considering only the $LS_{0.3}$MO as a magnetic active layer. From the calculated dM_S/dT we can identify the antiferrodistortive transition of the STO as well as the Curie temperature for both samples. A single magnetic transition at 288 K is observed for the ML_{STO} and two transitions (135 K and 340 K) are

visible for the ML_{LMO}. The transition at low and high temperatures corresponds to the Curie temperature of the LMO and $LS_{0.3}MO$ respectively. It is noteworthy that the magnetization and Curie temperature of the ML_{STO} at low temperatures are 2.8 μ_B/Mn and 288 K, well below the bulk values. The depleted magnetization values are reflecting an inhomogeneous and asymmetric magnetization profile within the $LS_{0.3}MO$, as we shall discuss later. In contrast, we note that the Curie temperature of the $LS_{0.3}MO$ in the ML_{LMO} is closer to the bulk value, which is also reflected in the magnetization profile reveal by polarized neutron reflectometry.

In Fig. 2(b) we show on the left an STEM-HAADF image of the ML_{STO} and on the right the strain map with the deformation of the structure along the z-axis (which corresponds to variations of the out of plane cell parameter *c* relative to a reference length) and the lattice deformation along the in-plane axis a / a_{STO}, obtained with the Geometrical Phase Analysis software. The chemical contrast of the STEM image shows sharp interfaces with absence of any notorious interdiffusion features. We first point out that the out of plane deformation correlates well with the periodicity of the structure, where the unit cell size along the z-axis for the regions corresponding to the STO layers is larger to the unit cell size beyond these regions. This is expectable considering that the STO has a larger unit cell parameter than the $LS_{0.3}MO$ and therefore it grows on the $LS_{0.3}MO$ with its structure extended along the z-axis. We also note that the structural deformation along the vertical axis is nearly uniform across the horizontal direction. Based on the this observation and using the deformation maps along the horizontal axis obtained with GPA (not shown in this graph), we averaged the deformation along the horizontal axis and calculated the ratio between the out of plane unit cell *c* and the well known STO cell parameter of the substrate, $c = a$ =3.905 Å (c / c_{STO}), which is displayed superimposed to the STEM image.

The most important feature to stress here is that the out of plane cell parameter of the $LS_{0.3}MO$ layers closed to the interface (between 2 and 3 nm) with the STO keep similar values to those observed for the STO. We distinguish a continuous variation of the out of plane parameter of the $LS_{0.3}MO$, where the minimum takes place closed to the middle of the layer. We also note that the in plane lattice parameter presents a profile consistent with the periodicity of the structure, although in this case the in plane unit cell relaxes abruptly at the interfaces (note that the structural deformation profile along the horizontal axis is 100 times smaller than the one obtained for the vertical deformation). We also performed EELS spectroscopy on the STEM images to reveal local changes in the composition and oxidation state of the elements. In this case we are particularly interested in the absorption L edge of the Mn, which results from the excitation of the 2p electrons into empty bound states or the continuum. Due to the spin orbit interaction two transitions can be observed at the L edge, namely the L_3 and L_2 which correspond to the transitions $2p_{3/2} \rightarrow 3d$ and $2p_{1/2} \rightarrow 3d$ respectively. The intensity ratio between these edges $L_3/L_2 = L_{23}$ increases with the number of electrons in the 3d bands of the Mn. In this context, it is expectable to find higher values of the L_{23} where the ratio Mn^{3+}/Mn^{4+} is larger. We calculated the L_{23} ratio for the STEM image shown in Fig. 1(b) and displayed the results superimposed to the image. We clearly see that the Mn^{3+}/Mn^{4+} ratio diminishes as we approach to the top interface. This electronic inhomogeinity could be a consequence of the non equilibrium thermal and mechanical conditions sustained during growth.

Polarized neutron reflectometry curves were measured at 150 K, after field-cooled the samples from room temperature with a magnetic field of 3 kOe applied parallel to the sample plane, thereby eliminating contributions from spin–flip scattering. This temperature was chosen as it is slightly above the Curie temperature of the LMO and maximizes the magnetic moment of the $LS_{0.3}MO$. We examined the non-spin flip scattering reflections, where the incident and scattered neutrons were polarized either spin-up or spin-down with respect to the applied in-plane magnetic field. The resulting spin dependent neutron specular reflectivities are sensitive to the depth profile of the in plane magnetization. The chemical and magnetic depth profiles were extracted from the simultaneous fitting of the x-ray reflectivities and PNR curves, based on a model that considers a periodic chemical profile and non-periodic magnetic profile throughout the multilayer, with a non-homogeneous magnetization within each $LS_{0.3}MO$ layer. The simultaneous fitting with GenX using the Parratt formalism ensures the consistency of both techniques. The model proposed has been kept as simple as possible, in order to minimize the number of fitting parameters and to obtain a reasonable fit of the data (in term of χ^2). Based on the structural and chemical results already discussed, here we proposed a model with two $LS_{0.3}MO$ sub-layers within each $LS_{0.3}MO$ layer. Even though the magnetization of these sub-layers were considered as independent parameters, the sum of their thicknesses must coincide with the chemical thickness given by the $LS_{0.3}MO$. In order to reduce the number of parameters even further, the fitting models considers that the overall magnetization must agree with those measured with the SQUID at that temperature and the magnetization of each $LS_{0.3}MO$ layer should not be larger than the bulk value of 3.7 μ_B/Mn.

In a conventional XRR measurement, the scattering length density depends on scattering factors sensitive to the chemical composition. In contrast, the reflectivity obtained with neutrons includes a nuclear contribution sensitive to the chemical structure of the material and a magnetic one, which is proportional to the local magnetization. In order to verify the robustness of our results, we started the fitting from different initial conditions and verified that in all cases the solution converge to the same SLD profile.

Fig. 2(a) and (b) show the observed spin dependent reflectivities R± (Q) as a function of the wave vector transfer Q and the resulting magnetization profile obtained for the reference sample ML_{STO}. The most notable finding here is the strongly asymmetric magnetization profile observed within the $LS_{0.3}MO$, with sharp magnetic contrast and large magnetization values at the bottom $LS_{0.3}MO$ interfaces, which decreases almost continuously across the $LS_{0.3}MO$ layer until it reaches the upper $LS_{0.3}MO$ interface with negligible magnetization. The asymmetry becomes more pronounce as we approach to the surface. The magnetic profile correlates fairly well with the profile observed for the Mn^{3+}/Mn^{4+}, where the interface with more electrons available on the 3d bands gives rise to a larger interfacial magnetization.

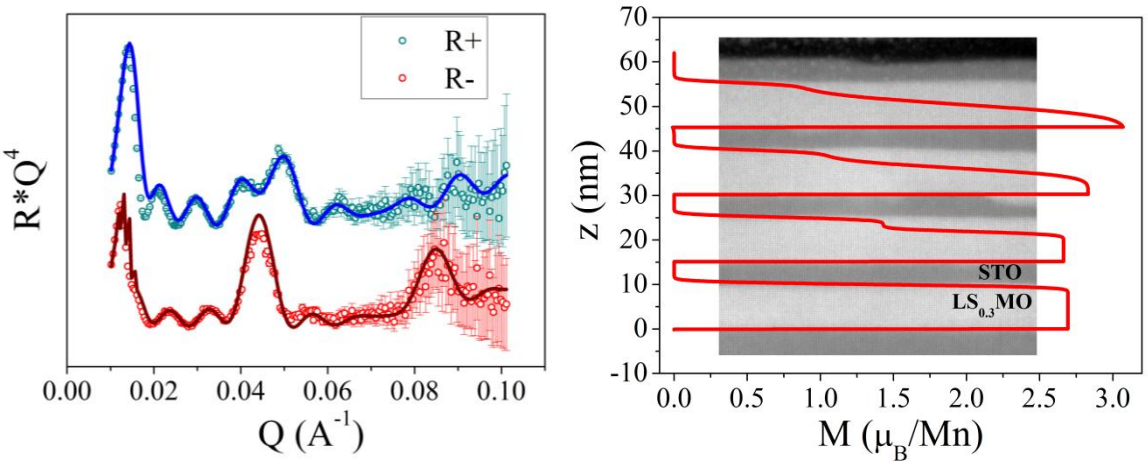

Fig. 2: (a) PNR (b) magnetization profile of the ML_{STO}.

We analyze now the results obtained for the sample ML_{LMO}. The corresponding magnetic profile is shown in Fig. 3(a) and 5(b), joint with the fittings of the neutron data. In this case the magnetic profile is more homogeneous within the $LS_{0.3}MO$ layer.

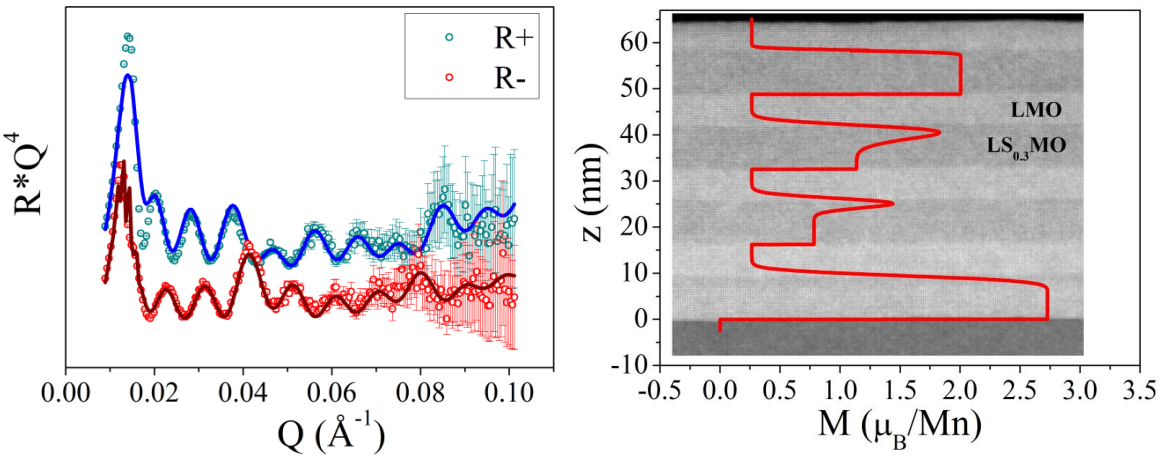

Fig. 3: (a) PNR (b) magnetization profile of the ML_{LMO}